A Pseudo Shock Theory of Pressure Depression in Externally Pressurized Circular Thrust Gas Bearings

AUTHOR(S):

MORI, Haruo; MURAKAMI, Kiyotaka

CITATION:

MORI, Haruo ...[et al]. A Pseudo Shock Theory of Pressure Depression in Externally Pressurized Circular Thrust Gas Bearings. Memoirs of the Faculty of Engineering, Kyoto University 1972, 34(4): 393-412

ISSUE DATE:

1972

URL:

http://hdl.handle.net/2433/280899

A Pseudo Shock Theory of Pressure Depression in Externally Pressurized Circular Thrust Gas Bearings

By

Haruo MORI* and Kiyotaka MURAKAMI**

(Received June 27, 1972)

Abstract

A theoretical investigation of the supersonic pressure depression in externally pressurized circular thrust gas bearings is developed with a pseudo shock wave model which replaces the concentrated normal shock wave model used in the previous paper[1].

The pseudo shock theory on the basis of appropriate assumptions used by Crocco can explain the gradual recovery of pressure after supersonic expansion flow from a single central supply hole.

Nomenclature

A = cross sectional area
a = sonic velocity
c_p = specific heat at constant pressure
F = function of r (region I)
f = friction facter
g = function of r (region I)
H = enthalpy flux
h = bearing clearance
I = momentum flux
J = impulse function
k = ratio of specific heats
M = Mach Number
m = dimensionless velocity
p = pressure (absolute)
q = mass rate of flow
R = outer bearing radius
$\mathfrak{R}$ = gas constant
Rey = Reynolds Number
r = radial position
r, θ, z = cylindrical coordinates
T = absolute temperature
u = velocity component in radial direction
$\bar{u}$ = temporal mean of velocity u in turbulent flow
W = external bearing load
δ = boundary layer thickness
δ^* = momentum thickness
μ = coefficient of viscosity
ν = coefficient of kinematic viscosity
ρ = density
τ = shear stress
$\Phi = \sqrt{(k-1)/(k+1)}$

* Department of Mechanical Engineering, II
** Sumitomo Shipbuilding & Machinery CO., LTD.

Subscripts

a=ambient
$avg.$=average
w=wall
x=preceding pseudo shock
y=following pseudo shock
o=bearing supply hole
I=supersonic region
II=pseudo shock region
III=subsonic region
∞=free stream

Superscripts

*=critical condition
°=stagnation condition
~=nondimension
′=central main flow
″=flow in dissipative region

1. Introduction

One of the important problems of externally pressurized gas bearings is the entrance effects which yield a sharp depression in the pressure profile near the supply hole. One of the authors presented a supersonic analysis on the pressure depression with concentrated normal shock wave when the gas flow is choked at the inlet to the circular thrust bearing with central supply hole[1]. The assumption of the occurence of the normal shock was used in order to simplify the problem and perform the theoretical analysis as an initial attack, although the actual flow in the clearance region was predicted to have a transition region from supersonic to subsonic one being accompanied by generation of a series of shock waves which might contain both normal and oblique components. Therefore, the analytical solution could not explain the gradual recovery of the pressure obtained experimentally in the transition region. It was quite meaningful at this point that Gross[2] explained, "There may be a normal shock in addition to the oblique shocks. The diffusion of the shocks through the boundary layers results in a gradual pressure increase. This aspect of the problem has not yet been solved analytically."

During the past several years, precisely this aspect of the problem has been studied as pseudo shock problems of the supersonic flow in ducts in the field of fluid mechanics. In this paper, the authors attempt to solve the pressure depression problem of the circular thrust bearing by introducing a pseudo shock model which is based on the shockless model for the flow in ducts by Crocco[3]. Since the pseudo shock is extremely difficult to analyse because of the complicated internal phenomenon, the shockless model by Crocco, which does not consider the entropy increase due to shock waves but takes into account the entropy increase due to the dissipation near the walls, is chosen as the simplest one. A few addi-

tional adaptations for the shockless model are used to apply it to the radial flow in the circular thrust bearing.

2. Assumptions

1. The circular thrust bearing treated in this paper has a constant film thickness and no recess as shown in Fig. 1. The gas with constant pressure p_0 is fed into a central hole which offers no restrictions to the flow.

2. The flow in the clearance space consists of three parts, region I with supersonic velocities, region II with a pseudo shock and region III with subsonic velocities.

3. The gas enters into region I with sonic velocity and critical pressure corresponding to the supply pressure.

4. The flow in region I is adiabatic one with predominant inertia force as assumed in the previous paper[1].

5. On the flow in region II, the assumptions are as follows according to the shockless model by Crocco;

a. The entropy increase due to a number of oblique shocks can be neglected, but the entropy increase due to the turbulence generated in the dissipative region near the walls is taken into account.

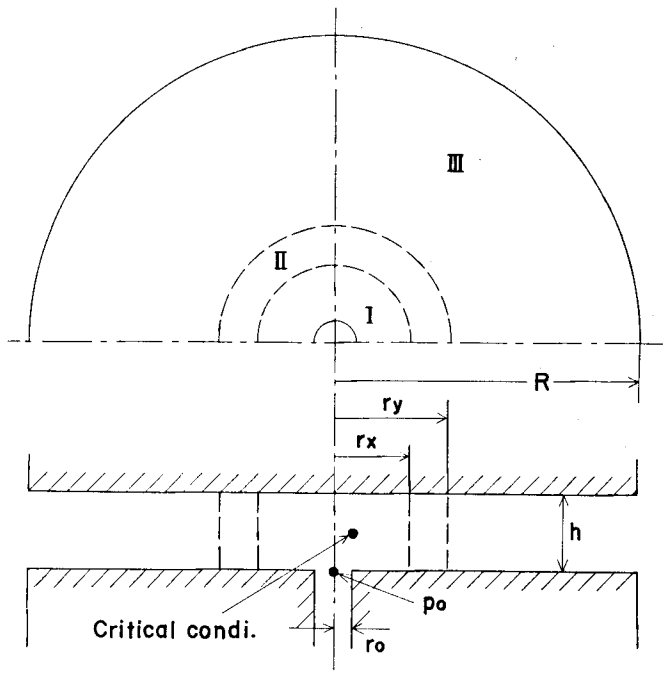

Fig. 1. Schematic diagram of circular thrust bearing

b. The central main flow is isentropic and has uniform velocities.

c. The nonuniform velocity in the dissipative region can be replaced with an approximately equivalent uniform velocity. The friction force on the walls is assumed to be negligible. The heat transfer from the walls is also negligible. The spreading rate of the dissipative region is assumed to be equal to that of the turbulent boundary layer with no pressure gradiant.

d. The pressure across the gas film is constant.

6. The flow in region III is a purely viscous and isothermal one.

3. Pressure Distribution

a. Region I.

In this region, as assumed above, viscosity has a negligible effect on the velocity distribution, in that the velocity is assumed constant across the clearance. However, the shear stress exerted on the stream by the walls is taken into account as was done in the previous paper[1]. The shear stress by the walls may be given experimentally by a function of Reynolds Number, but in the following, it is assumed constant for convenience of calculation. The results are summarized as follows;

velocity:

$$m \equiv u/a^* = \left(\frac{2}{k+1}\right)^{\frac{1}{k-1}} p^{-\frac{1}{k}} \tilde{r}^{-1}, \tag{1}$$

pressure:

$$\frac{\tilde{p}}{\tilde{p}^*} = \left(\frac{k^2-1}{F^2-1}\right)^{\frac{1}{2}} \tilde{r}^{-1}, \tag{2}$$

where F is determined by radial position r;

$$\frac{1}{2(k-1)} \ln\left[\left(\frac{F^2-1}{k^2-1}\right)^{k+1}\left(\frac{k-1}{F-1}\right)^{2k}\right] = \ln \tilde{r} - \frac{k}{2}\frac{fr_0}{h} g(\tilde{r}), \tag{2-1}$$

$$g(\tilde{r}) = (\tilde{r}-1) - 2.58(\tilde{r}-1)^{\frac{5}{4}} + 4.77(\tilde{r}-1)^{\frac{3}{2}} - 0.08(\tilde{r}-1)^2. \tag{2-2}$$

f in the equation (2-1) is the friction factor defined by $f = 2\tau_w/\rho_\infty u_\infty^2$.

b. Region II

In order that the supersonic flow in region I decreases its velocity to that of the subsonic flow in region III, shock waves should be generated. Since the boundary layers at walls increase their thickness rapidly, a series of X-type shocks waves may be generated when the Mach Number is large enough[4]. On behalf of the interference between the shock waves and the boundary layers, the boundary layers spread into the central main flow, which leads to the entropy increase.

In the following analysis the entropy increase due to the shock generations is assumed small compared with that due to the dissipation caused by the inter-

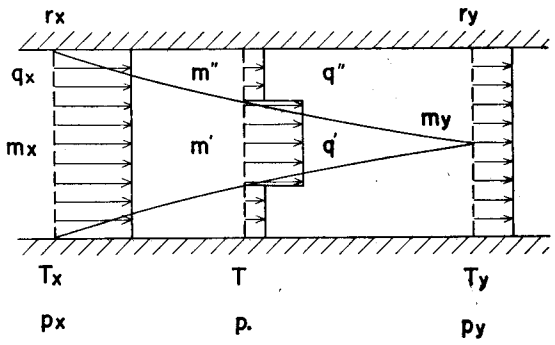

Fig. 2. Definition of control volume.

ferences according to Crocco who has successfully analysed one dimensional flow in ducts. Since the flow in the clearance of the bearing is radial one, we should analyse the problem by taking into account the effect of area change.

The control volume to be considered is a circular ring of which cross section is rectangular as shown in Fig. 2.

In this case, from the condition of continuity,

$$q'+q''=q_x,$$

and from the energy conservation, (assumption 5.c)

$$q'H'+q''H''=q_xH_x.$$

At $r=r_x$, the initial section of the pseudo shock region, the central main flow occupies the whole clearance space, and this means $H_x=H'$. Using these relations, we obtain

$$H'=H''=H_x$$

Since $H=c_pT^\circ$ and the specific heat at constant pressure c_p is constant for perfect gas, the stagnation temperature is therefore the same throughout the flow. Thus,

$$T^{\circ\prime}=T^{\circ\prime\prime}=T_x^\circ, \tag{3}$$

from which we obtain

$$c_pT+u^2/2=c_pT^\circ.$$

Since the flow in region II is adiabatic one, we have

$$c_p=k/(k-1)\cdot\Re,\quad a^{\circ 2}=k\Re T^\circ,\quad a^{*2}/a^{\circ 2}=2/(k-1).$$

Using these equations we have the relation between absolute temperatures and dimensionless velocities:

$$T/T^\circ=1-\Phi^2m^2. \tag{4}$$

In the following we will reduce the continuity equation into a more convenient form. Using equation of state of perfect gas $p/\rho=\Re T$, mass rate of flow through a cross sectional area A can be written as

$$q=pA/\Re T\cdot u \tag{5}$$

From the definition of dimensionless velocities:

$$u=ma^*=m\sqrt{k\Re T^*},$$

and the relation $T^\circ/T^*=\frac{k+1}{2}$ for adiabatic flow, we have

$$u=\sqrt{\frac{2k}{k+1}}\,m\sqrt{\Re T^\circ}. \tag{6}$$

Substituting equations (4) and (6) into equation (5) yields

$$q=\frac{pA}{\sqrt{\Re T^\circ}}\sqrt{\frac{2k}{k+1}}\,\frac{m}{1-\Phi^2m^2}, \tag{7}$$

from which we obtain a continuity equation:

$$pA'\frac{m'}{1-\Phi^2m'^2}+pA''\frac{m''}{1-\Phi^2m''^2}=p_xA_x\frac{m_x}{1-\Phi^2m_x^2}.$$

Since $A=2\pi rh$ for this bearing, we finally arrive at a working dimensionless form of the continuity equation as follows;

$$\frac{h'}{h}\frac{m'}{1-\Phi^2m'^2}+\frac{h''}{h}\frac{m''}{1-\Phi^2m''^2}=\frac{\tilde r_x}{\tilde r}\frac{\tilde p_x}{\tilde p}\frac{m_x}{1-\Phi^2m_x^2}. \tag{8}$$

The flow in the dissipative region is so slow that the shear stress can be successfully neglected in the momentum equation[3]. In this case the momentum equation is

$$[I+pA]_{r_x}^{r}=\int_{A_x}^{A}pdA, \tag{9}$$

where momentum flux I is

$$I=\frac{A}{h}\int_0^h\rho u^2dz. \tag{9-1}$$

Both the central main flow region and the dissipative region have uniform velocities (assumptions 5.b and 5.c), so the integration of equation (9–1) can be easily performed in each region to become

$$I=qu. \tag{10}$$

(Although there is no superscript in equation (10), we must write superscript ′ or ″, depending on which region we are concerned with.) Using equations (6) and (7), the impulse function $J=I+pA$ can be written as

$$I+pA=pA\frac{1+m^2}{1-\Phi^2m^2}. \tag{11}$$

From equations (9) and (11) we have

$$p'A'\frac{1+m'^2}{1-\Phi^2m'^2}+p''A''\frac{1+m''^2}{1-\Phi^2m''^2}-p_xA_x\frac{1+m_x^2}{1-\Phi^2m_x^2}=\int_{A_x}^{A}pdA.$$

Using $A=2\pi rh$, $dA=2\pi hdr$, $p=p'=p''$ (assumption 5.d) and dimensionless variables, we have a working form of the momentum equation as follows:

$$\frac{h'}{h}\frac{\tilde p}{\tilde p_x}\frac{1+m'^2}{1-\Phi^2m'^2}+\frac{h''}{h}\frac{\tilde p}{\tilde p_x}\frac{1+m''^2}{1-\Phi^2m''^2}-\frac{\tilde r_x}{\tilde r}\frac{1+m_x^2}{1-\Phi^2m_x^2}=\int_1^{\frac{1}{r_x}}\frac{\tilde p}{\tilde p_x}d\left(\frac{\tilde r}{\tilde r_x}\right). \tag{12}$$

Since the central main flow is isentropic, that is, $T^\circ/T=(p^\circ/p)^{\frac{k-1}{k}}$, the equation (4) can be written as

$$\frac{p^\circ}{p}=\left(\frac{1}{1-\Phi^2m^2}\right)^{\frac{k}{k-1}},$$

which leads to a relation between variables in the initial section and the arbitrary section:

$$\frac{\tilde{p}}{\tilde{p}_x}=\left(\frac{1-\Phi^2m'^2}{1-\Phi^2m_x^2}\right)^{\frac{k}{k-1}}. \tag{13}$$

In a wide range of Mach Numbers, the experimental length of the pseudo shock in a circular tube is around 10 times of the tube diameter, which is nearly equal to the spreading length of the ordinary turbulent boundary layer. The spreading rate of the dissipative region can be, therefore, replaced by the corresponding rate at which the turbulent boundary layer with no pressure difference spreads[3]. In order to analyse the turbulent boundary layer we must take into account the shear stress on the walls, which was neglected in the equation (9). Falkner[5] has shown the following empirical friction law for turbulent flow;

$$\frac{\tau_w}{\rho u_\infty^2}=0.0131\,\mathrm{Rey}^{-\frac{1}{7}}\quad\left(\mathrm{Rey}=\frac{u_\infty r}{\nu}\right) \tag{14}$$

where u_∞ is a constant free stream velocity.

The integral momentum equation of the turbulent boundary layer is obtained by using the momentum thickness δ^*;

$$\frac{\tau_w}{\rho u_\infty^2}=\frac{1}{r}\frac{\partial}{\partial r}(r\delta^*), \tag{15}$$

where

$$\delta^*=\int_0^\delta\frac{\bar{u}}{u_\infty}\left(1-\frac{\bar{u}}{u_\infty}\right)dz.$$

The velocity profile within the turbulent boundary layer is given by the $\frac{1}{7}$-th-power law of velocity distribution[6], that is

$$\bar{u}/u_\infty=(z/\delta)^{\frac{1}{7}},$$

which gives the relation between the momentum thickness and the boundary layer thickness;

$$\delta^*=7/72\cdot\delta. \tag{16}$$

From equations (14), (15) and (16), we obtain

$$0.1347\left(\frac{\nu}{u_\infty r}\right)^{\frac{1}{7}}r=\frac{\partial}{\partial r}(r\delta).$$

Integration from the initial value $\delta=0$ at $r=r_x$ gives

$$\delta=\frac{9}{125}\left(\frac{u_\infty}{\nu}\right)^{-\frac{1}{7}}(r^{\frac{13}{7}}-r_x^{\frac{13}{7}})\frac{1}{r}.$$

Using equality $\delta=h''/2$ (assumption 5.c) and dimensionless variables, we obtain

$$\frac{h''}{h}=\frac{18}{125}\left(\frac{a^*h}{\nu}\right)^{-\frac{1}{7}}\left(\frac{r_0}{h}\right)^{\frac{6}{7}}\frac{\tilde{r}^{\frac{13}{7}}-\tilde{r}_x^{\frac{13}{7}}}{\tilde{r}}m', \tag{17}$$

and then,

$$\frac{h'}{h}=1-\frac{h''}{h}. \tag{18}$$

The equation (17) gives the spreading rate of the dissipative region. We assume that the pseudo shock region will vanish when the dissipative region at both sides of the central main flow occupies the whole clearance space. Therefore, the vanishing position of the pseudo shock region renders $h''=h$ or $h'=0$.

c. Region III.

In the region after the psuedo shock, the flow is assumed a purely viscous and isothermal one, with negligible inertia effects as was assumed in the previous paper[1];

mean velocity:

$$m_{avg.}=\frac{h^3p_0}{24\mu a^*r_0}\frac{1}{\tilde{r}\ln(\tilde{R}/\tilde{r}_y)}\frac{\tilde{p}_y^2-\tilde{p}_a^2}{\tilde{p}} \tag{19}$$

pressure:

$$\left(\frac{\tilde{p}}{\tilde{p}_y}\right)^2=1-\left\{1-\left(\frac{\tilde{p}_a}{\tilde{p}_y}\right)^2\right\}\frac{\ln(\tilde{r}/\tilde{r}_y)}{\ln(\tilde{R}/\tilde{r}_y)} \tag{20}$$

4. Boundary Condition

The continuity of the pressure and the mass rate of flow at the boundary between region I and region II gives the following equations, using equations (1) and (2);

$$m_x=\left(\frac{2}{k+1}\right)^{\frac{1}{k-1}}\tilde{p}_x^{-\frac{1}{k}}\tilde{r}_x^{-1}, \tag{21}$$

$$\frac{\tilde{p}_x}{\tilde{p}^*}=\left(\frac{k^2-1}{F_x^2-1}\right)^{\frac{1}{2}}\tilde{r}_x^{-1}, \tag{22}$$

where

$$\frac{1}{2(k-1)}\ln\left[\left(\frac{F_x^2-1}{k^2-1}\right)^{k+1}\left(\frac{k-1}{F_x-1}\right)^{2k}\right]=\ln\tilde{r}_x-\frac{f}{2}\frac{r_0}{h}g(\tilde{r}_x), \tag{22-1}$$

$$g(\tilde{r}_x)=(\tilde{r}_x-1)-2.58(\tilde{r}_x-1)^{\frac{5}{4}}+4.77(\tilde{r}_x-1)^{\frac{3}{2}}-0.08(\tilde{r}_x-1)^2. \tag{22-2}$$

At the boundary between region II and region III, the mass rate of flow must be kept continuous. From equation (19) we obtain

$$m_y=\frac{h^3p_0}{24\mu a^*r_0}\frac{1}{\tilde{r}_y\ln(\tilde{R}/\tilde{r}_y)}\frac{\tilde{p}_y^2-\tilde{p}_a^2}{\tilde{p}_y}. \tag{23}$$

The equations (8), (12) and (13) can be written as following at the position

$r=r_y$:

$$\frac{m_y}{1-\Phi^2 m_y^2}=\frac{\tilde{r}_x}{\tilde{r}_y}\frac{\tilde{p}_x}{\tilde{p}_y}\frac{m_x}{1-\Phi^2 m_x^2}, \tag{24}$$

$$\frac{\tilde{p}_y}{\tilde{p}_x}\frac{1+m_y^2}{1-\Phi^2 m_y^2}-\frac{\tilde{r}_x}{\tilde{r}_y}\frac{1+m_x^2}{1-\Phi m_x^2}=\int_1^{\frac{r_y}{r_x}}\frac{\tilde{p}}{\tilde{p}_x}d\left(\frac{\tilde{r}}{\tilde{r}_x}\right), \tag{25}$$

$$\frac{\tilde{p}_y}{\tilde{p}_x}=\left(\frac{1-\Phi^2 m_y'^2}{1-\Phi^2 m_x^2}\right)^{\frac{k}{k-1}}. \tag{26}$$

At the vanishing position of the pseudo shock ($h''=h$ at $r=r_y$), equation (17) can be written as

$$\tilde{r}_y^{\frac{13}{7}}-\frac{125}{18}\left(\frac{a^*h}{\nu}\right)^{\frac{1}{7}}\left(\frac{h}{r_0}\right)^{\frac{6}{7}}m_y'\tilde{r}_y-\tilde{r}_x^{\frac{13}{7}}=0. \tag{27}$$

Since the right hand side of the equation (25) includes an integration of unknown variable p, it cannot, in general, be integrated in a closed form. Since the pressure distribution in region II has an almost linear profile when measured, we assume it to be linear as a first approximation:

$$\tilde{p}-\tilde{p}_x=(\tilde{p}_y-\tilde{p}_x)/(\tilde{r}_y-\tilde{r}_x)\cdot(\tilde{r}-\tilde{r}_x). \tag{28}$$

Then the integration of equation (25) gives

$$\frac{1+m_y^2}{1-\Phi^2 m_y^2}-\frac{\tilde{p}_x}{\tilde{p}_y}\frac{\tilde{r}_x}{\tilde{r}_y}\frac{1+m_x^2}{1-\Phi^2 m_x^2}=\frac{1}{2}\left(1+\frac{\tilde{p}_x}{\tilde{p}_y}\right)\left(\frac{\tilde{r}_y}{\tilde{r}_x}-1\right). \tag{29}$$

When the operating conditions and the bearing dimensions are given, the first approximation of the unknown variables r_x, r_y, p_x, p_y, m_x, m_y, m_y', are obtained by the equations (21), (22), (23), (24), (26), (27) and (29).

These results are next used to obtain the second approximation of the pressure distribution; we can calculate the right hand side of equation (12) by the first approximation, that is, eq. (28), then equations (8), (12), (13), (17) and (18) render the second approximation pressure profile. Higher ones would be obtained through the same procedure.

The pressure distributions in region I and region III are given by equations (2) and (20) respectively.

5. Load Capacity

The load capacity can be calculated by the integration of the pressure distributions in region I, region II and region III.

It is, however, quite difficult to integrate the pressure distribution in region I based on equation (2). Therefore, an approximate evaluation, assuming the friction facter f equals zero, is used.

$$W_I=\pi r_0^2 p_0[\{3.64\ln\tilde{r}_x-7.12(1-\tilde{r}_x^{-1}) +2.73(1-\tilde{r}_x^{-2})+1.90\}\tilde{p}^*-\tilde{r}_x^2\tilde{p}_a] \tag{30}$$

The load capacity in region II is given approximately by the integration of the linear pressure distribution of the first approximation;

$$W_{II}=\pi/3\cdot r_0^2 p_0(\tilde{r}_y-\tilde{r}_x)\{(2\tilde{r}_y+\tilde{r}_x)\tilde{p}_y+(\tilde{r}_y-2\tilde{r}_x)\tilde{p}_x-3(\tilde{r}_y+\tilde{r}_x)\tilde{p}_a\}. \quad (31)$$

In region III an approximate solution is also used. For convenience of calculation, the pressure distribution is assumed to be that of an incompressible fluid.

$$W_{III}=\pi r_0^2 p_0(\tilde{p}_y-\tilde{p}_a)\left\{\frac{\tilde{R}^2-\tilde{r}_y^2}{2\ln(\tilde{R}/\tilde{r}_y)}-\tilde{r}_y^2\right\} \quad (32)$$

Consequently, the approximate load carried by the bearing will be

$$W=W_I+W_{II}+W_{III}. \quad (33)$$

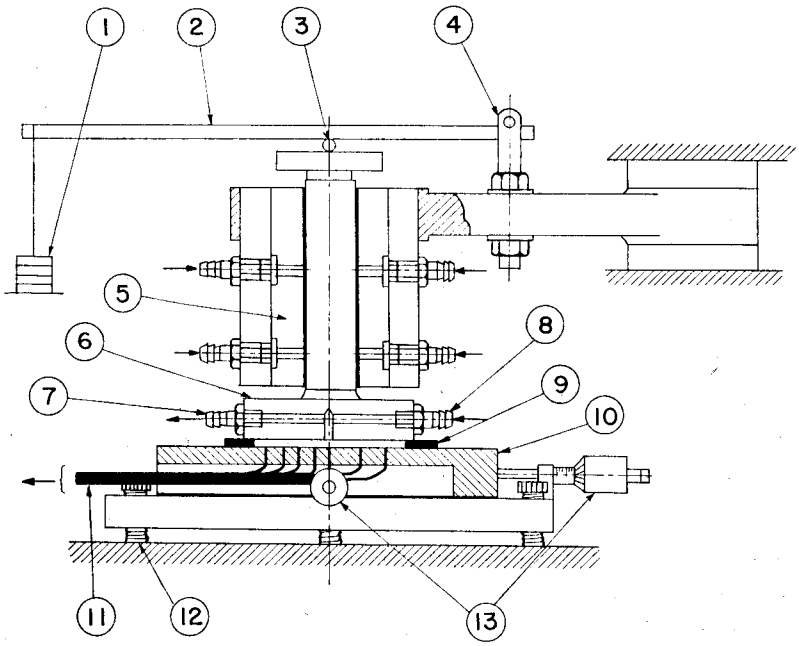

1	dead weight	8	nipple for supplying air to thrust bearing
2	loading lever		
3	steel ball	9	thickness gauge
4	lever support	10	thrust bearing plate
5	journal air bearing	11	pressure measuring tubes
6	thrust plate	12	adjustable screws
7	nipple for measuring supply pressure	13	micrometer screws

Fig. 3. Apparatus for experiment.

6. Comparison with Experimental Results

a. Apparatus and Method of Experiment.

Some experiments were carried out in order to compare them with the theoretical results. The apparatus for the experiment is shown schematically in Fig. 3. The floater had a thrust bearing surface with a single central supply hole through which compressed air was supplied into the bearing clearance, and had a jounal bearing surface which was guided in the outer sleeve without contact.

The pressure distribution was measured by U-tube mercury manometers and Burdon tube manometers which were connected to the clearance space through small holes with 0.3 mm diameter drilled at 2 mm interval on the stator. The stator could be moved by a fine screw to measure the entire pressure distribution on the bearing surface. The bearing clearance was measured by a dial gage at first, but it was quite difficult to make the bearing clearance perfectly uniform. The thickness gages were, therefore, inserted into the outer edge of bearing to

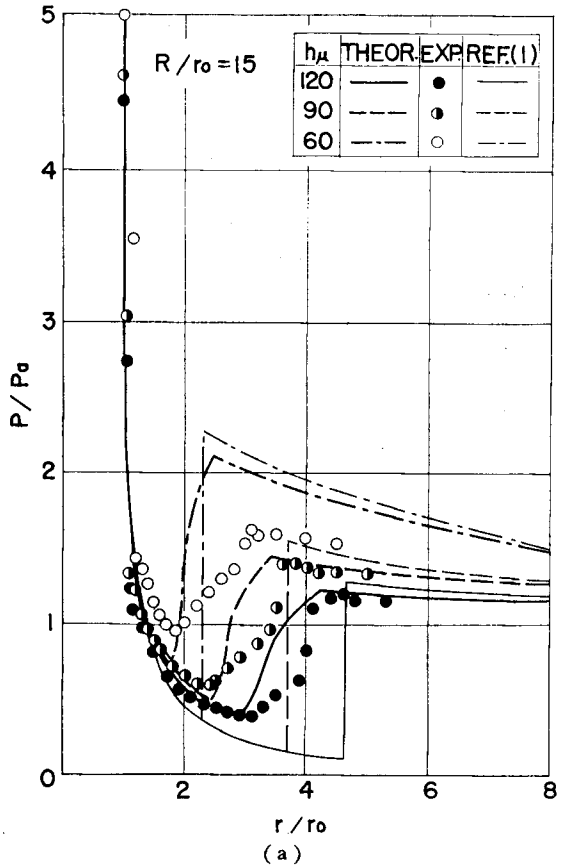

(a)

make the bearing clearance perfectly uniform. Thus, it was impossible to know the load capacity directly.

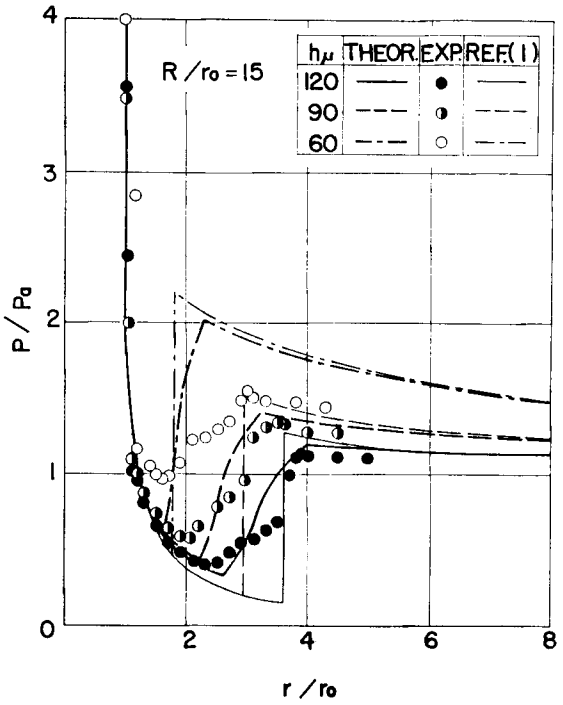

(b)

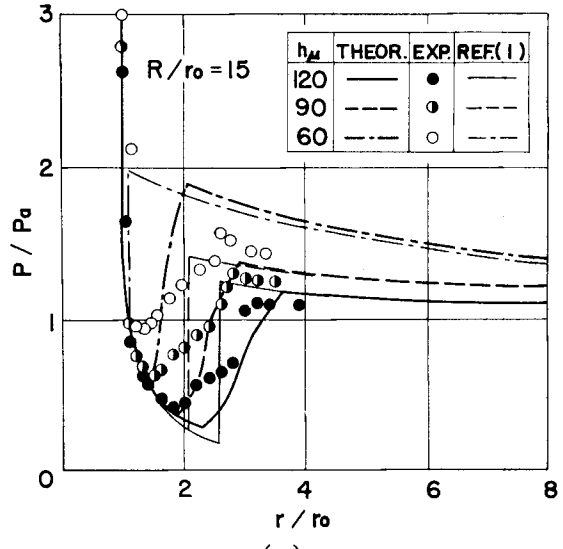

(c)

Fig. 4. Pressure distribution ($R/r_0 = 15$).

b. Pressure Distribution.

Fig. 4 (a), (b), (c), and Fig. 5 (a), (b), (c) show the experimental and theoretical pressure distributions near the supply hole for $R/r_0=15$ and 30 respectively. The theoretical pressure distribution in region I was calculated by assuming $f=0.003$. In an actual case, the friction factor has a large value at the entrance to the clearance space, getting smaller with increasing velocities in region I. The above value of f is reasonably chosen as their mean[2][4].

The theoretical and the experimental results agree well in both the subsonic and supersonic region. The gradual pressure recovery in the transition region is explained well by the pseudo shock theory, although the theoretical pressure profiles by the previous normal shock theory, which are shown by thin chain curves in the figures, fail entirely to follow the experimental data in the transition region.

c. Minimum Pressure, Recovered Pressure.

Fig. 6 (a) and (b) show the minimum pressure and the recovered pressure in

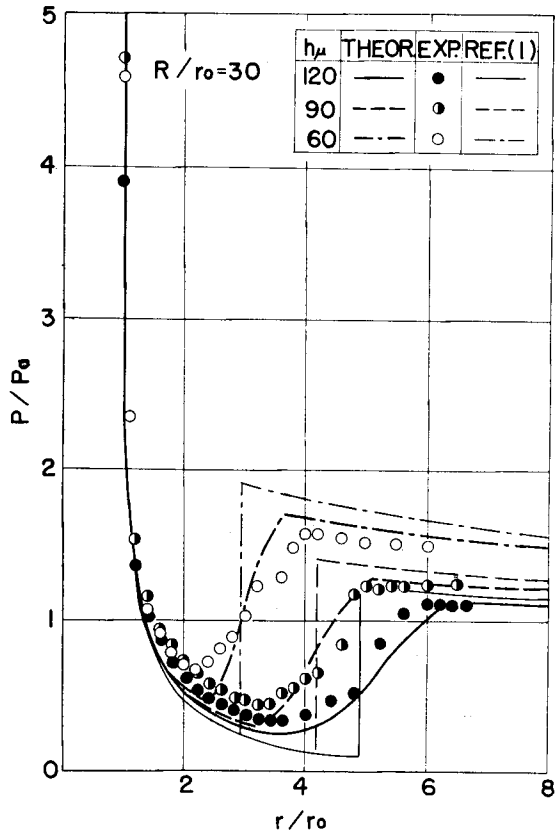

(a)

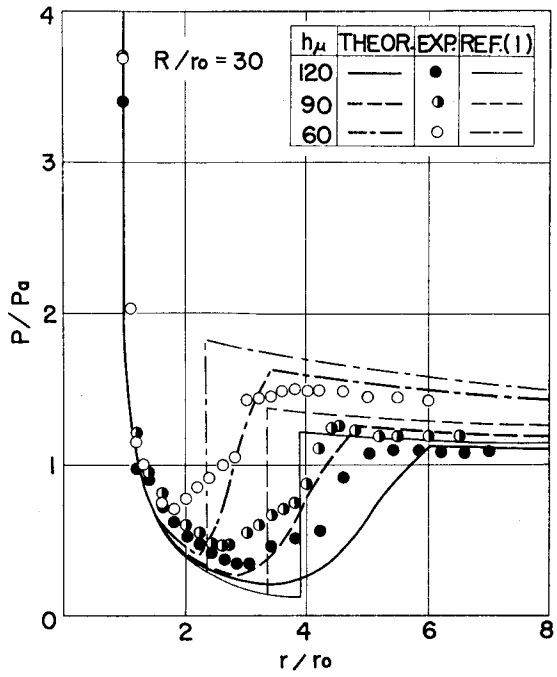

(b)

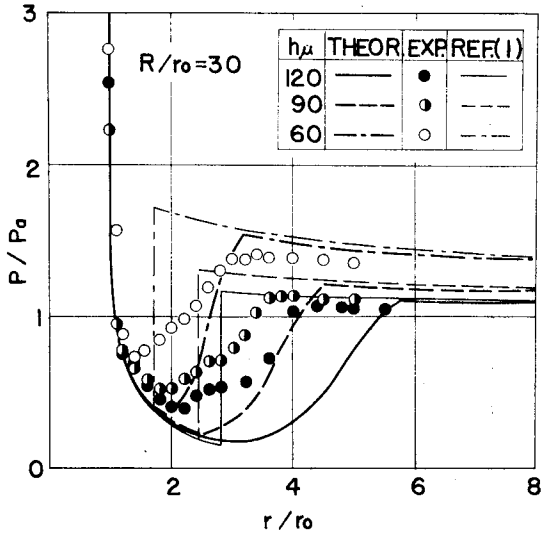

(c)

Fig. 5. Pressure distribution ($R/r_0=30$).

the clearance region versus the supply pressure for $R/r_0=15$ and 30 the bearing clearance h being fixed as parameter.

The theoretical and experimental results agree well qualitatively, but not

quantitatively. The discrepancy may consist in the rather large radius of the pressure measuring taps and in the roundness of the supply hole edge, which could not be removed in the present experiment.

The larger theoretical recovered pressure compared to the experimental re-

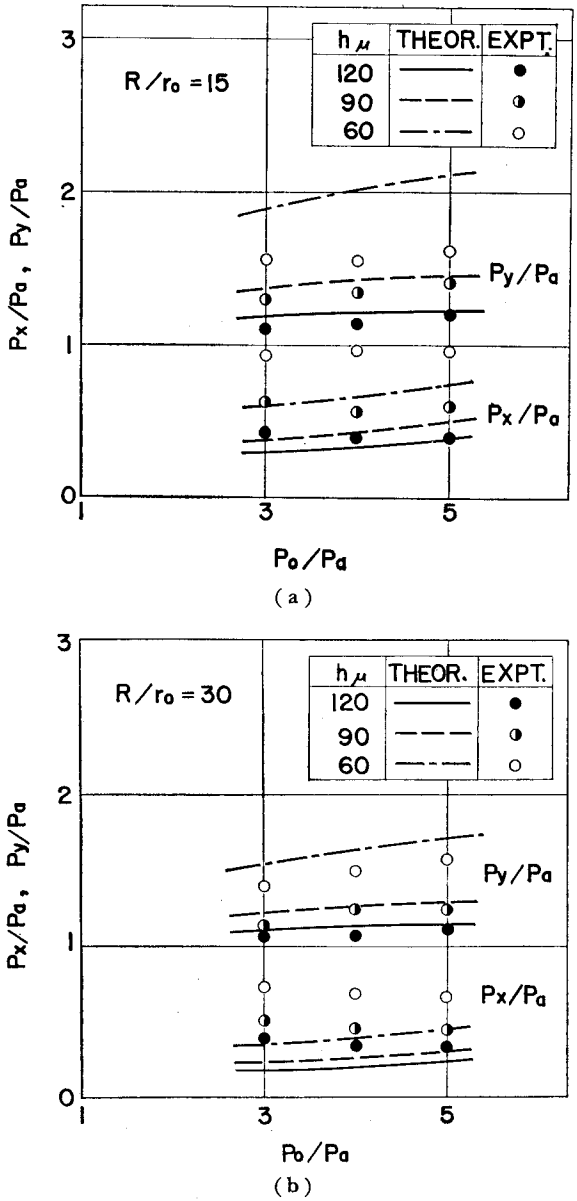

Fig. 6. Minimum pressure and recovered pressure versus supply pressure, theoretical and experimental.

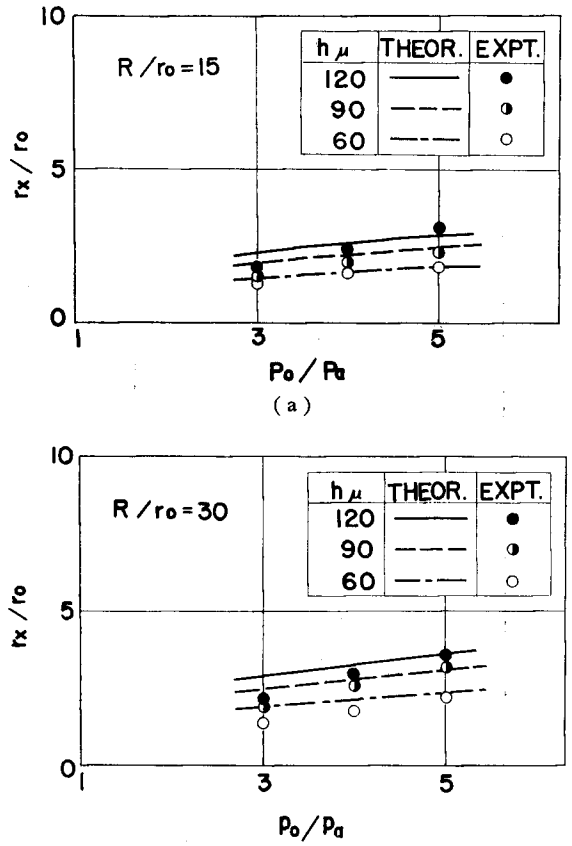

Fig. 7. Starting position of transition region versus supply pressure, theoretical and experimental.

sults would partly be due to the neglected entropy increases by the shock waves.

d. Starting Position of Transition Region.

In Fig. 7 (a) and (b) the starting position of the transition region II for $R/r_0=15$ and 30 are shown, the bearing clearance h being fixed as parameter.

The figures manifest qualitative agreement between the experimental results and the theoretical ones.

e. Vanishing Position of Transition Region.

The experimental results of the vanishing position of the transition region II are compared with the theory when R/r_0 is equal to 15 and 30 in Fig. 8 (a) and (b).

The quite gradual pressure recovery near the boundary between regions II and III makes the experimental results deviate from the theoretical ones, since

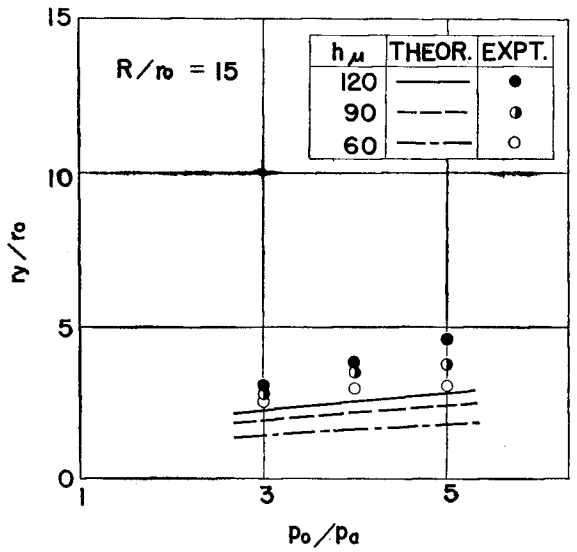

Fig. 8. Vanishing position of transition region versus supply pressure, theoretical and experimental.

it was quite difficult to determine the vanishing position in the experiment, owing to the rather large radius of pressure measuring taps, although we obtained qualitative agreement between the experimental results and the theoretical ones.

f. Width of Transition Region.

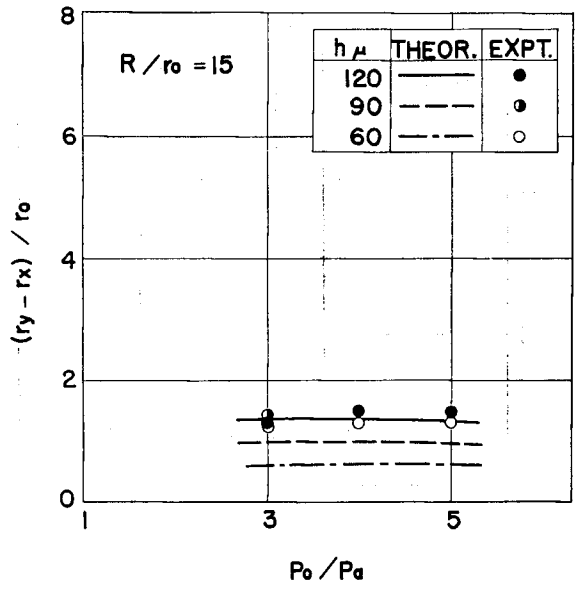

Fig. 9. Length of transition region versus supply pressure, theoretical and experimental.

Fig. 9 (a) and (b) indicate the experimental and theoretical width of the transition region II for $R/r_0=15$ and 30 respectively.

The experimental results show that the dimensionless width of the transition

region increases with the ratio R/r_0 and the bearing clearance h while it would hardly be influenced by the supply pressure.

g. Load Capacity.

Fig. 10 (a) and (b) indicate the comparison between the load capacities based on the present pseudo shock theory and on the normal shock theory[1], the horizontal coordinate being the supply pressure, with the bearing clearance h as parameter.

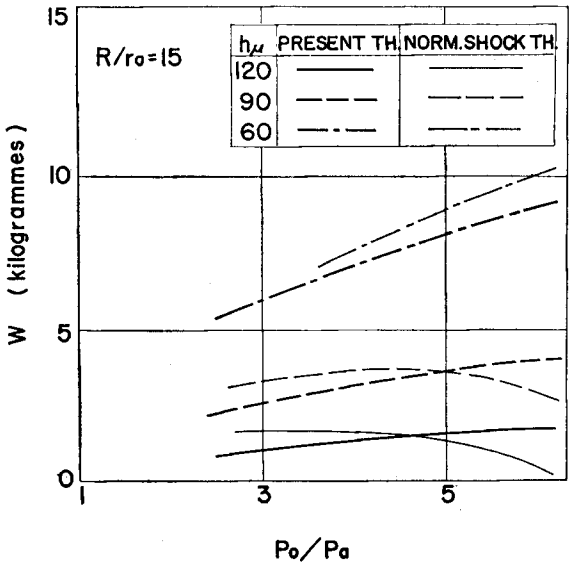

(a)

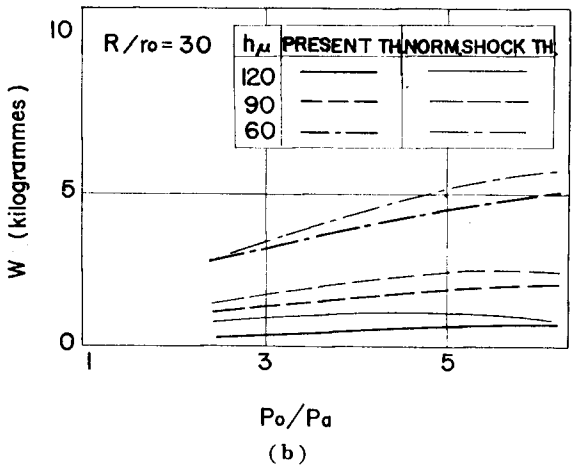

(b)

Fig. 10. Load capacity versus supply pressure, comparison with normal shock theory[1].

The present pseudo shock theory gives less load capacity than the normal shock theory in low supply pressures, which is easily understood from the transition region being taken into account in the pseudo shock theory. The load capacity based on the present theory increased with the supply pressure within the pressure range of the figures, while that based on the normal shock theory shows decreased with increasing supply pressure.

h. Discontinuity in the Present Theory.

In region II, the flow near the walls is accelerated by mixing with the central main flow. The velocity of the dissipative region, therefore, should become equal to that of the central main flow when the mixing is over at the end of region II. In this report, however, it is assumed that the pseudo region will end when the dissipative region occupies the whole clearance space. At the vanishing position of the pseudo shock region, there exists some amount of difference between the velocities of the central main flow region and dissipative region.

At the boundary between regions I and II, the shear stress in region II does not agree with the mean shear stress in region I, the precise analysis being left for the future.

7. Conclusion

The degree of qualitative agreement between theoretical and experimental pressure distributions and pressure ratios indicates that the basic concept of pseudo shock generation in clearance space is valid, with the quantitative discrepancies being due to the simplifications made in the construction of the mathematical model.

It would appear that further theoretical refinements should deal with the supersonic and transition regions with more precision, removing the unrealistic assumption of the constant shear stress in the supersonic region, although such a solution would be difficult.

Bibliography

1) H. Mori: "A Theoretical Investigation of Pressure Depression in Externally Pressurized Gas-Lubricated Circular Thrust Bearings", Trans. ASME, Vol. 83, Series D, No. 2, June 1961, pp. 201–208.
2) W. A. Gross: "Gas Film Lubrication", John Wiley and Sons Inc. New York (1962).
3) L. Crocco: "High Speed Aerodynamics and Jet Propulsion", Princeton Univ. Press. Vol. III, Series B (1958), p. 110.
4) T. Tamaki, Y. Tomita and R. Yamane: "A Research on Pseudo Shock (2nd Rep., X-type Pseudo Shock)", Trans. JSME, Vol. 36, No. 292, Dec. 1970, pp. 2056–2066. (Japanese).
5) V. N. Falkner: "A New Law for Calculation Drag", Air-craft Engineering, Vol. 15, No. 169, 1943, p. 65.